DynamITE: Optimal time-sensitive organ offers using ITE

Alessandro Marchese* ALESSANDRO.MARCHESE@VUB.BE
Vrije Universiteit Brussel, Belgium

Hans de Ferrante H.DEFERRANTE@EUROTRANSPLANT.ORG
Eurotransplant International Foundation, Leiden, the Netherlands

Jeroen Berrevoets JEROEN.BERREVOETS@MATHS.CAM.AC.UK
University of Cambridge, England

Sam Verboven SAM.VERBOVEN@VUB.BE
Vrije Universiteit Brussel, Belgium

Abstract

Matching donor organs to patients in need is a difficult but important problem. A crucial factor in transplant outcomes is the cold ischemic time of the organ, which increases every time an organ offer is refused. Despite this, acceptance dynamics have so far been neglected in favor of purely outcome driven offers. As a first alternative, we propose DynamITE, a novel organ allocation methodology that explicitly takes into account the acceptance behavior over sequences of offers. DynamITE dynamically updates organ acceptance estimates, cold ischemic times (CIT) and causal effects throughout the matching process. We demonstrate that DynamITE improves early organ acceptance and maximizes patient life expectancy compared to current policies.

Keywords: Organ allocation, Individual treatment effects, Decision making

Data and Code Availability The organ-patient pair data reported in section 5 has been supplied by the United Network for Organ Sharing as the contractor for the Organ Procurement and Transplantation Network. The interpretation and reporting of the data are the responsibility of the author(s) and in no way should be seen as an official policy of or interpretation by the OPTN or the U.S.Government.

The code used to generate the synthetic data and for the experiments is made available on https://github.com/AlessandroMarchese/DynamITE.

Institutional Review Board (IRB) As stated above, our paper only uses publicly available data, or simulated data, and hence does not require an IRB approval.

1. Introduction

Organ transplantation is the only curative therapy for patients with end-stage organ disease. However, due to a persistent donor shortage in the United States 17 patients die every day while waiting for a transplant (HRSA, 2023). Simultaneously, almost 20 percent of the organs recovered for transplantation in the United States remain unused (Israni et al., 2024). There is an urgent need for organ allocation systems that efficiently place the limited supply of available organs to meet the increasing demand for transplantation and ultimately improve clinical outcomes.

Turndowns of organ offers degrade organ quality and lead to organ nonuse. Transplant centers frequently decline offered organs on behalf of their patients, for instance because of logistical or donor quality reasons (Mulvihill et al., 2020; Goldberg et al., 2016). In fact, in the United States organ offer acceptance rates are only 1% for kidneys, 3% for livers, and 5% for hearts (OPTN and SRTR, 2024). Moreover, most transplanted organs are declined by multiple patients before transplantation. Such repeated turndowns of an organ and delays in offer acceptance decisions mean that the organ has to be kept longer in a hypothermic state (King et al., 2021; Wey et al., 2017). These extended Cold Ischemic Times (CIT) are detrimental to the quality of the organ, and negatively affect transplant outcomes (Debout

* Corresponding author(s)

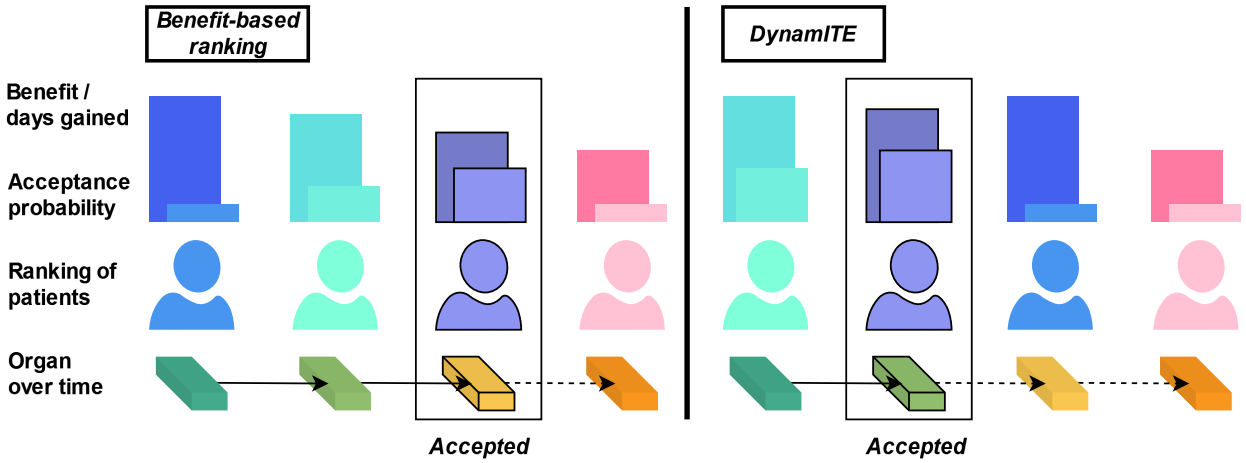

Figure 1: **Problem setting.** The benefit of an organ diminishes over time. Consequently, the more an organ is refused and passed down, the lower the probability of it being accepted and the lower the ultimate benefit for the patient who eventually accepts it. DynamITE takes into account decision time and the probability of acceptance, enhancing the overall benefit by promoting earlier acceptance of organs. In contrast, a policy that disregards acceptance probability (left) will yield a reduced benefit compared to DynamITE (right).

et al., 2015). Additionally, delays in acceptance decisions and repeated turndowns lead to organ nonuse (Mohan et al., 2018; Stewart et al., 2017).

Existing allocation policies ignore offer turndowns. Current organ allocation systems prioritize candidates based on scores for medical urgency (Wiesner et al., 2003) or anticipated transplant benefit (Allen et al., 2024; Egan et al., 2006). Lists of waiting candidates ranked in this way are referred to as *match-runs*. These match-runs determine the order in which candidates are offered the organ until a candidate accepts the organ for transplantation. Currently, a candidate's likelihood of accepting the graft offer does not affect their position on the match-run. As shown in figure 1, this may lead to repeated turndowns, extend CITs, and consequently lead to worse transplant outcomes.

To avoid nonuse of transplantable organs, organ allocation organizations have implemented ad hoc mechanisms that allow them to deviate from the match-run in case nonuse is anticipated (Vinkers et al., 2009; King et al., 2022; White et al., 2015). For instance, such organs may be offered with priority to centers with aggressive offer acceptance policies (Hackmann et al., 2022). Although such "out-of-sequence" offering may indeed reduce nonuse, it has been criticized for lacking transparency (Husain et al., 2023) and exacerbating geographical inequities (King et al., 2022).

Nonuse of transplantable organs could instead be avoided more transparently and fairly by basing a candidate's match list position also on their estimated offer turndown risk (in addition to medical urgency or anticipated benefit). This could increase placement efficiency and reduce nonuse rates of transplantable organs, which is the explicit aim of the '*Expeditious Task Force*', which was initiated in 2023 the United States to reduce organ nonuse.

Challenges in optimizing match-runs. Incorporating offer organ acceptance behavior and its impact on CIT into the design of organ matching policies is inherently complex for several reasons. First, precise predictions are needed regarding how long patients will live after receiving a particular organ. This coincides with the individualized treatment effect (ITE) estimation challenge in organ transplantation (Berrevoets et al., 2020, 2021). Second, organ acceptance behavior is highly stochastic, and depends on extensive sets of patient and donor characteristics (Wood et al., 2021). Finally, the sequential nature of the organ allocation process introduces a sequential bias to ITE estimation (Gomez et al., 2023). This is because acceptance behavior upstream in the allocation process directly affects which organ offers

downstream candidates receive, and negatively impacts quality of the organ through CIT.

Correcting for this bias is particularly difficult, as each decision influences not only the quality of the organ (due to cold ischemic time) but also the potential benefits for downstream patients. These dynamics make optimizing match-runs a fundamentally different and more challenging problem than what existing policies are equipped to address.

Our contribution: DynamITE. In this paper, we present DynamITE, a novel organ allocation methodology that optimizes organ-to-patient matching by incorporating ITEs while accounting for the sequential and time-sensitive nature of organ offers. Unlike existing models that assume matches are always and instantaneously accepted, DynamITE uses predicted offer acceptance probabilities and decision times to dynamically update organ offers, taking into account adjusted CIT with each successive offer. This innovation ensures more timely acceptance decisions, reducing CIT and preventing organ nonuse. We demonstrate DynamITE's effectiveness through a series of experiments on semi-synthetic data (real patient-organ pairs with synthetic outcomes), showing substantial improvements in patient life expectancy and reduced CITs compared to other policies.

2. Related work.

Organ allocation policies. Currently used match-runs in organ transplantation prioritize candidates based on medical urgency or anticipated benefit. For instance, MELD (Malinchoc et al., 2000) and MELD-Na (Kim et al., 2008) are scoring functions for medical urgency, which have been used to prioritize candidates for liver transplantation. MELD-based match-runs fail to capture complex interactions between organs and other patients that influence patient outcomes. Policies have been proposed based on a causal approach, relying on potential outcomes and ITE to rank patients (Neuberger et al., 2008; Yoon et al., 2017). Additionally, some policies take operational aspects of transplantation into consideration, such as arrival rates of other organs and patients (Berrevoets et al., 2020, 2021) or the transport distance (Ata et al., 2017; Bertsimas et al., 2020). Thus far, no policies have been proposed that explicitly take the operational aspect of acceptance uncertainty into consideration, leading DynamITE to be the first policy to explicitly model acceptance uncertainty and its effect on CIT.

Offer acceptance modeling. Discrete event simulators are routinely used for policy evaluation in transplantation (SRTR, 2015a,b, 2019). The goal of such simulators is to mimic the complete organ allocation process, which includes waitlist survival, generation of match-runs, and simulation of post-transplant survival (Sandikci et al., 2019). A key component of such simulators are modules that predict organ offer acceptance decisions based on patient and donor characteristics (Wood et al., 2021). The widely used models developed by the Scientific Registry of Transplant Recipients (SRTR) rely on logistic models for making offer acceptance predictions (SRTR, 2015b,a, 2019). Others have explored basing these prediction models on traditional ML methods (Kim et al., 2015; Bertsimas et al., 2017), or more complex conditional acceptance rules based on organ-patient compatibility (Zhang et al., 2023). Importantly, organs are treated as static objects in such simulations, ignoring the deterioration of donor quality through increased CITs due to repeated turndowns. In DynamITE, spillover effects of repeated offer turndowns on organ quality are accounted for, as well as explicitly optimized over.

3. Problem formulation.

The organ allocation process consists of an organ being repeatedly offered to candidates on a waitlist until a candidate accepts the organ. We model three aspects of this allocation process: the order (match-run) in which an organ is offered to waitlist candidates, how candidates respond to an organ offer, and how long waitlist candidates and transplant recipients survive. A summary of all introduced notation can be found in table 6 in appendix C.

Responding to offers. Let $\mathcal{X} \subset \mathbb{R}^d$ be the space of all possible patients and $\mathcal{O} \subset \mathbb{R}^e$ the space of all possible organs. When an organ $\mathbf{O} \in \mathcal{O} \cup \{\emptyset\}$ is offered to a patient $\mathbf{X} \in \mathcal{X}$, we observe a response $A \in \{0, 1\}$, where $A = 1$ if the offer is accepted, and $A = 0$ if it is refused. The time between offer and response is denoted $T \in \mathbb{R}_+$.

Sequential offers. Consider $\mathcal{X}_Q \subset \mathcal{P}(\mathcal{X})$ as a waiting list of size $K = |\mathcal{X}_Q|$. As an organ is offered sequentially to different patients and deteriorates over time, consider $\mathbf{O}_k$ as the organ offered to $\mathbf{X}_k \in \mathcal{X}_Q$

where $k \in \mathbb{Z}^+$ represents a sequence number and $1 \leq k \leq K$. Similarly, A_k and T_k represent the answer and decision time of patient $\mathbf{X}_k$ when faced with the offer of organ $\mathbf{O}_k$. When a donor organ becomes available this initial organ $\mathbf{O}_1 \in \mathcal{O}$ must be matched with a patient in the waiting list.

Consider $\mathbf{R} \in \text{Sym}(\mathcal{X}_Q)$ as a ranking of wait-listed patients, representing a match-run. When a donor organ becomes available, a policy π attributes a rank k to each patient in $\mathcal{X}_Q$ such that $\mathbf{R} = (\mathbf{X}_k)_{k=1}^K$.

A patient $\mathbf{X}_P$ who accepts the offer $A_P = 1$ will receive the transplant. Organs are offered to patients following the ranking $\mathbf{R}$ in ascending order until a patient $\mathbf{X}_P$ for which $A_P = 1$ is found, meaning that all patients before rank P refused the offer: $\forall k < P : A_k = 0$ and all patients after rank P do not receive an offer $\forall k > P : \mathbf{O}_k = \emptyset$

Transplant outcomes. Following Berrevoets et al. (2020), we define $Y^{\mathbf{o}}$ as the potential life expectancy for a patient $\mathbf{X}$ when they receive the organ from an accepted offer $\mathbf{o} \in \mathcal{O} \cup \{\emptyset\}$. If $\mathbf{o} = \emptyset$, it signifies the scenario where the patient does not receive an organ and thus dies before a transplant. Let $Y = Y^{\mathbf{O}}$ be the resulting observed outcome. An accepting patient $\mathbf{X}_P$ receives the organ $\mathbf{O}_{P+1}$ that would have been offered to the next patient $\mathbf{X}_{P+1}$, as T_P affects the received organ where the expectation is taken over the acceptance rates and the decision times. The organ matched with a patient $\mathbf{X}$ under policy π is denoted as $\mathbf{O}_{\mathbf{X}}^{\pi} \in \mathcal{O} \cup \{\emptyset\}$.

Let $\tau(\mathbf{X}, \mathbf{O}) = \mathbb{E}[Y^{\mathbf{O}} - Y^{\emptyset} \mid \mathbf{X}]$ be the ITE or benefit of a patient $\mathbf{X}$ who receives the organ $\mathbf{O} \in \mathcal{O}$ and let $\tau_k = \tau(\mathbf{X}_k, \mathbf{O}_k)$. We define the benefit of a ranking $\mathbf{R}$ as the benefit of the patient who accepts $\tau(\mathbf{R}, \mathbf{O}_1) = \sum_{k=1}^K \tau_k \mathbb{I}[A_k = 1]$ which simplifies to $\tau(\mathbf{R}, \mathbf{O}_1) = \tau_P$ for observed runs. Finally, consider $\kappa(\mathbf{R}, \mathbf{O}_1) = \mathbb{E}[\tau(\mathbf{R}, \mathbf{O}_1)]$ as the expected benefit from a ranking and an initial organ, where the expectation is taken over the patient distribution $p(\mathbf{X})$ and the initial organ distribution $p(\mathbf{O}_1)$.

Training data. We use a dataset containing offers for donor organs alongside with patients' acceptance. A set of offers is observed for each new organ. Formally, $\mathcal{D} = \{((\mathbf{x}_k, \mathbf{o}_k, a_k, t_k) : k = 1, ..., P_i) : i = 1, ..., N\}$ where N is the total number of initial offers and each tuple $(\mathbf{x}_k, \mathbf{o}_k, a_k, t_k)$ is generated by the patient distribution $p(\mathbf{X})$, the initial organ distribution $p(\mathbf{O}_1)$ and the executed policy π_{obs}.

Objective. The primary objective is to develop and validate a policy that optimizes the allocation and acceptance of organ offers in a dynamic and time-sensitive context. Specifically, given a dataset $\mathcal{D}$ that includes historical organ offers, patient characteristics, and their responses, the goal is to identify a ranking policy $\hat{\pi} : \mathcal{X}_Q \times \mathcal{O} \to Sym(\mathcal{X}_Q)$ that maximizes the expected benefit κ, where the expectation of the benefit is taken over the distributions of patient attributes $p(\mathbf{X})$ and initial organ offers $p(\mathbf{O}_1)$. The challenge lies in ensuring that the policy not only ranks patients in a way that maximizes their individual treatment effects (ITE) but also takes into account the stochastic nature of patient decisions.

The performance of a policy is measured (in experiment 5.2) based on the following measures: the expected ITE, the expected rank of the accepting patient, the expected final CIT of the organ and the percentage of nonused organs.

Assumptions. In the context of using an ITE estimator to test different policies, the three core assumptions of causal inference will have to be made: positivity and unconfoundedness (Berrevoets et al., 2020), and the Stable Unit Treatment Value Assumption (SUTVA).

Assumption 1 (Positivity.)

$$\forall \mathbf{x} \in \mathcal{X}, \mathbf{o} \in \mathcal{O} : 0 < P(\mathbf{o}|\mathbf{x}) < 1 \tag{1}$$

Positivity assumes that we have sufficient data across all types of organs for all types of patients.

Assumption 2 (Unconfoundedness.)

$$\mathbf{O}_{\mathbf{X}}^{\pi_{obs}} \perp\!\!\!\perp \{Y^{\mathbf{o}} : \mathbf{o} \in \mathcal{O}\} \mid \mathbf{X} \tag{2}$$

Under unconfoundedness, the full set of potential outcomes should be independent of the factors that influence organ assignment, after controlling for patient covariates.

Assumption 3 (SUTVA.) Sequential bias, which originates from compounding decision times that affect CIT, violates SUTVA (Gomez et al., 2023). SUTVA assumes that (i) for each patient, there are no hidden treatment variations, which lead to different potential outcomes, and (ii) the potential outcomes for one patient are independent of the treatment assignments of other patients. In this case, however, the decision time of one patient impacts the organ offer for others, leading to dependent outcomes. Modeling sequential offers considering the organ as a static

object would violate SUTVA, resulting in spillover effects which would lead to inaccurate estimations. In section 4.1 we describe how we respect this assumption in the context of sequential organ offers.

4. DynamITE.

DynamITE is composed of four key components: a mechanism that dynamically updates organ offers, a decision time estimator, an offer acceptance estimator, and an ITE estimator. By integrating these components, DynamITE is able to create a feasible search space that facilitates the identification of the optimal ranking for organ allocation.

4.1. Updating organ offers.

Due to the sequential nature of the matching process, SUTVA is violated, causing dependencies between the outcomes (A_k, T_k) of the patient at rank k and the patients $\mathbf{X}_n$ with rank n lower than k and their corresponding organ offers $\mathbf{O}_n$. Specifically, we want the path from previous offers, patients and outcomes to be closed, ensuring the necessary conditional independence:

$$A_k, T_k \perp\!\!\!\perp \{\mathbf{X}_n, \mathbf{O}_n : n \in [1; k-1]\} \mid \mathbf{X}_k, \mathbf{O}_k \quad (3)$$

To achieve this, we rely on a set U_F of update rules to keep the offers up to date in the simulations, and ensure that outcomes are solely dependent on the patient receiving the offer and the offer itself:

$$U_F := \{\forall f \in F : \mathbf{O}_{k+1}[f] := g_f(\mathbf{O}_k, \hat{T}_k)\}, \quad (4)$$

where F consists of a set of features that are time dependent, f is a feature, $\hat{T}_k$ is the estimated decision time of patient $\mathbf{X}_k$ for offer $\mathbf{O}_k$ and $g_f(\mathbf{O}_k, \hat{T}_k)$ is a function that models how feature f depends on time. Consider u_F as a function applying this set of updates, we can then define and assume the structural causal relationship:

$$\mathbf{O}_{k+1} := u_F(\mathbf{X}_k, \mathbf{O}_k) \quad (5)$$

Applying u_F updates the time dependent features of an organ offer. Recursively applying u_F will result in further $\mathbf{O}_k$ estimates, for example:

$$\mathbf{O}_3 := u_F(\mathbf{X}_2, u_F(\mathbf{X}_1, \mathbf{O}_1)). \quad (6)$$

Conditioning on the updated offer, the path from previous offers, patients and outcomes is closed, ensuring the necessary conditional independence 3.

We only consider CIT as feature in F as it is the main time dependent feature of an organ. We set $g_{\text{CIT}}(\mathbf{O}_k, \hat{T}_k) := \mathbf{O}_k[\text{CIT}] + \hat{T}_k$, this will result in the CIT of an organ to be updated, after each patient answer, throughout a sequence of offers.

4.2. PatientNet.

In order to update the organ after each offer and to estimate offer acceptance we train a model that jointly estimates decision time and the acceptance probability in a multi-task fashion. Consider PatientNet, shown in figure 2, as an estimator with parameters θ_Φ, θ_T and θ_A for: the shared representation, $\phi = \Phi_{\theta_\Phi}(\mathbf{X}, \mathbf{O})$; the decision time, $\hat{T} = T_{\theta_T}(\phi)$; the acceptance probability, $\hat{A} = A_{\theta_A}(\phi)$. We define a Mean Squared Error loss ($\mathcal{L}_{MSE}$) for $\hat{T}$ and a binary cross-entropy loss ($\mathcal{L}_{BCE}$) for $\hat{A}$ such that the total loss $\mathcal{L}_{PatNet}(\theta_\Phi, \theta_T, \theta_A)$ becomes:

$$\mathcal{L}_{MSE}(\theta_\Phi, \theta_T) + \gamma \mathcal{L}_{BCE}(\theta_\Phi, \theta_A) \quad (7)$$

where γ is a hyperparameter controlling the trade-off between the different prediction tasks. We seek the saddle point $(\theta^*_\Phi, \theta^*_T, \theta^*_A)$ by solving the following optimization problem:

$$(\theta^*_\Phi, \theta^*_T, \theta^*_A) := \arg\min_{\theta_\Phi, \theta_T, \theta_A} \mathcal{L}_{PatNet}(\theta_\Phi, \theta_T, \theta_A) \quad (8)$$

These parameters are learned by minimizing $\mathcal{L}_{PatNet}(\theta_\Phi, \theta_T, \theta_A)$ using stochastic gradient descent-based optimization.

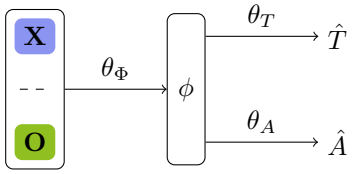

Figure 2: **PatientNet Architecture**: the patient $\mathbf{X}$ and organ $\mathbf{O}$ vectors are concatenated. A representation ϕ is learned across both estimation tasks. The output of the model is the estimated decision time $\hat{T}$ and the estimated acceptance probability $\hat{A}$. Patient and organ color codes are the same as the match made by DynamITE in figure 1.

4.3. DynamITE policy.

The objective. In section 3, we defined $\kappa(\mathbf{R}, \mathbf{O}_1)$ as the expected τ corresponding to a match-run.

Now, given that each patient has a certain probability of accepting the offered organ, we can achieve a closed-form expression for $\kappa(\mathbf{R}, \mathbf{O}_1)$:

$$\kappa(\mathbf{R}, \mathbf{O}_1) = \sum_{k=1}^{K} \tau_k P(A_k = 1 | \mathbf{R}, \mathbf{O}_1) \tag{9}$$

The probability of a proposed transplant taking place $P(A_k = 1|\mathbf{R}, \mathbf{O}_1)$ is further broken down into two factors: (i) the probability of the organ being offered to the patient, and (ii) the probability of the patient accepting the organ offer:

$$P(A_k = 1|\mathbf{X}_k, \mathbf{O}_k) \prod_{n=1}^{k-1} P(A_n = 0|\mathbf{X}_n, \mathbf{O}_n) \tag{10}$$

These acceptance probabilities, and the decision times of the patients, can then be jointly estimated using a PatientNet model and τ can be estimated by any ITE estimator: $\hat{\tau} = \tau_{\theta_\tau}(\mathbf{X}, \mathbf{O})$. Using the estimated values $\hat{\tau}_k$ and $\hat{A}_k$, we approximate $\kappa(\mathbf{R}, \mathbf{O}_1)$ as follows:

$$\kappa(\mathbf{R}, \mathbf{O}_1) \approx \sum_{k=1}^{K} \hat{\tau}_k \hat{A}_k \prod_{n=1}^{k-1} (1 - \hat{A}_n) \tag{11}$$

The optimization problem. Consider $\xi(\mathbf{R}, k)$ as a a function that returns $\mathbf{X}_k$ in $\mathbf{R}$. Suppose that τ can be estimated by any ITE estimator: $\hat{\tau} = \tau_{\theta_\tau}(\mathbf{X}, \mathbf{O})$. We can define DynamITE $\hat{\pi}(\mathcal{X}_Q, \mathbf{O}_1)$, a policy that maximizes a closed-form approximation of κ, as follows:

$$\underset{\mathbf{R} \in Sym(\mathcal{X}_Q)}{\arg\max} \quad \sum_{k=1}^{K} \hat{\tau}_k \hat{A}_k \prod_{n=1}^{k-1} (1 - \hat{A}_n) \tag{12}$$

$$\text{s.t.} \quad \hat{A}_k = A_{\theta_A}(\Phi_{\theta_\Phi}(\mathbf{X}_k, \hat{\mathbf{O}}_k)), \qquad \forall k \tag{13}$$

$$\hat{\tau}_k = \tau_{\theta_\tau}(\mathbf{X}_k, \hat{\mathbf{O}}_{k+1}), \qquad \forall k \tag{14}$$

$$\hat{\mathbf{O}}_{k+1} = u_F(\mathbf{X}_k, \hat{\mathbf{O}}_k), \qquad \forall k \tag{15}$$

$$\mathbf{X}_k \neq \mathbf{X}_{k'}, \qquad \forall k \neq k' \tag{16}$$

$$\mathbf{X}_k = \xi(\mathbf{R}, k), \qquad \forall k \tag{17}$$

$$\hat{\mathbf{O}}_1 = \mathbf{O}_1 \tag{18}$$

Here, constraint 13 models the acceptance probabilities using an updated organ estimate, constraint 14 models the estimated ITE using an updated organ estimate and constraint 15 is responsible for the organ updates. Constraints 16 and 17 represent ranking constraints. Constraint 16 ensures that no two patients in the ranking are assigned the same ranks while constraint 17 enforces that the ranking of patients is consistent with the order dictated by the policy.

Solving the optimization problem. To solve the optimization problem 12, we rely on a heuristic initialization to provide a high-quality starting point for a local search algorithm. DynamITE initializes a ranking by ranking the patients in ascending order using simple Dynamics Aware (Dyna) scores:

$$\text{Dyna}(\mathbf{X}, \mathbf{O}_1) := \frac{A_{\theta_A}(\Phi_{\theta_\Phi}(\mathbf{X}, \mathbf{O}_1))^{\alpha_A}}{T_{\theta_T}(\Phi_{\theta_\Phi}(\mathbf{X}, \mathbf{O}_1))^{\alpha_T}} \tau_{\theta_\tau}(\mathbf{X}, \mathbf{O}_1)^{\alpha_\tau}, \tag{19}$$

where $\alpha_A, \alpha_T, \alpha_\tau$ are tunable hyperparameters; representing the respective importance of acceptance, decision time and ITE. The initial ranking is then further improved using any local search algorithm. For our experiments, we use a local search based on adjacent swaps.

5. Experiments.

Additional experiments regarding DynamITE's search algorithm and a positivity assumption check can be found in A. Supplemental materials regarding synthetic functions, hyperparameters, the generation of scenarios, DynamITE and additional results can be found in appendix B. Information about the features used for the experiments can be found in appendix C.

5.1. PatientNet: Acceptance and decision time estimation.

Experimental setup. We create semi-synthetic training set $\mathcal{D}$ using real liver-patient pair data from the UNOS dataset (Cecka, 2000) with synthetic outcomes. Similarly to Berrevoets et al. (2020), we train two kernel density estimators (KDEs), one on patients and one on organs, and use them to generate new patient and organ vectors. We first generate a set of initial organs, meaning their CIT is set to 0, and for every organ we generate a set of patients which represents $\mathcal{X}_Q$. Since we are using data for livers, we rank patients according to their MELD scores. We construct a synthetic acceptance function based on organ-patient compatibility conditions (Zhang et al., 2023). These conditions, together with the numerical value of CIT and MELD will result in a score $\beta(\mathbf{X}, \mathbf{O})$ which will be turned into

Table 1: Performance metrics on $\mathcal{D}_{\text{test}}$ for acceptance (BCE, AUROC, AUPRC, and Brier score) and decision time (MSE) for different ML models. Standard deviation is reported in brackets next to each score.

Models	BCE	AUROC	AUPRC	Brier score	MSE
Linear Regression	n.a.	n.a.	n.a.	n.a.	.176 (.486)
Logistic Regression	.124 (.506)	.777	0.169	.029 (.144)	n.a.
SVM	.142 (.529)	.563	0.066	.031 (.157)	.192 (.698)
AdaBoost	.192 (.248)	.819	0.214	.039 (.101)	.103 (.254)
RF	.154 (1.613)	.889	0.419	.023 (.115)	.037 (.201)
PatientNet	**.067** (.298)	**.966**	**0.478**	**.019** (.090)	**.036** (.123)

an acceptance probability: $A = \sigma(\beta(\mathbf{X}, \mathbf{O}))$ (SRTR, 2019). We also construct a decision time function $T = \lambda A(1-A)\exp(-(A-\frac{1}{2})^2) + U_T$, with U_T being a uniform distribution. Both λ and the hyperparameters in β are tuned such that the average CIT of accepted organs and the average acceptance rates coincide with real statistics. Each simulated and observed tuple $(\mathbf{x}_k, \mathbf{o}_k, a_k, t_k)$ is added to $\mathcal{D}$. We then split $\mathcal{D}$ into a train and test set: $\mathcal{D}_{\text{train}}$ and $\mathcal{D}_{\text{test}}$ respectively. Finally, we train PatientNet on $\mathcal{D}_{\text{train}}$ such that it is able to predict acceptance probabilities and decision times.

Benchmarks. The methods we use as benchmarks are traditional ML methods that have been previously used to model acceptance (as discussed in section 2): linear regression, logistic regression (Kim et al., 2015; SRTR, 2019), Support Vector Machine (SVM), AdaBoost and Random Forests (RF) (Bertsimas et al., 2017). For each benchmark, 2 separate models are trained (if possible): one for acceptance and one for decision time. We train and compare different ML models on their performance in predicting the acceptance rate and decision time for a given organ-patient pair. As these models could be used to rank patients, we report the AUROC for the acceptance estimations.

Results. In table 1 we report the results which show that within the benchmarks, both Logistic Regression and Random Forests seem to be the best choices. However, PatientNet significantly outperforms all benchmarks on the acceptance metrics while being on par with Random Forests for predicting decision times.

5.2. DynamITE: Ranking patients.

ITE estimator. An OrganITE model (Berrevoets et al., 2020) is used as ITE estimator and is trained on real organ-patient pair data from the UNOS dataset (Cecka, 2000) combined with synthetic outcomes. However, we make sure that CIT has a negative effect on patient outcomes. The same OrganITE model is used for all policies that make use of an ITE estimator to keep the comparisons fair.

Benchmarks. We formulate the following benchmarks, $\pi(\mathcal{X}_Q, \mathbf{O}_1)$: (i) MELD (Malinchoc et al., 2000); (ii) MELD-Na (Kim et al., 2008); (iii) maximal acceptance (MaxAcc), which ranks the patients based on their estimated acceptance rate: $A_{\theta_A}(\Phi_{\theta_\Phi}((\mathbf{X}_k, \mathbf{O}_1))$ in descending order; (iv) minimal decision time (MinTime), which ranks the patients based on their estimated decision time: $T_{\theta_T}(\theta_\Phi(\mathbf{X}_k, \mathbf{O}_1)$ in ascending order, (v) TransplantBenefit (TB) (Neuberger et al., 2008), which ranks the patients based on their ITE: $\tau(\mathbf{X}_k, \mathbf{O}_1)$ in descending order. We compare the benchmarks with DynamITE, which searches for a ranking that maximizes κ. It is important to note that MELD and MELD-Na are organ invariant. While MaxAcc, MinTime and TB consider organ-specific features, they still only consider its initial features.

Experimental setup. We use the same KDEs from experiment 5.1 to generate initial organs and for each organ, a waiting list $\mathcal{X}_Q$. Next, we test each policy for each generated scenario and compute the average rank of the accepting patient (APTR), CIT, ITE and the percentage of nonused organs for each policy. Each benchmark has access to the trained OrganITE and PatientNet models however the mentioned metrics are obtained using the synthetic acceptance, decision time and OrganITE.

Table 2: Average ITE, acceptance rank, cold ischemic time and nonuse percentage for policies tested over 10 different runs of each of the 1000 KDE generated scenarios. Standard deviation is reported in brackets next to each score.

Policies	ITE (days gained)	APTR	CIT	Nonuse
MELD	926 (34)	9.36 (.22)	7.22 (.11)	21.8% (1.1%)
MELD-Na	939 (33)	9.66 (.32)	7.39 (.13)	22.7% (.7%)
MaxAcc	1097 (35)	**2.43** (.12)	**5.32** (.16)	**14.5%** (1.1%)
MinTime	684 (41)	26.07 (.64)	10.64 (.16)	31.4% (.9%)
TB (w/ OrganITE)	3429 (61)	9.86 (.25)	7.44 (.08)	22.5% (1%)
DynamITE	3515 (108)	7.71 (.32)	6.91 (.12)	21.3% (.7%)
DynamITE (w/ search)	**3582** (53)	7.87 (.26)	7 (.11)	21.9% (.9%)

Results. Table 2 shows the performance of the policies across the different metrics. The MaxAcc policy, maximizing acceptance, significantly reduces APTR, CIT and nonuse. However, this strategy is not effective in terms of ITE compared the ITE-based policies: TB and DynamITE. Paradoxically, MinTime results in the highest APTR, CIT and nonuse. This is because, on average, patients who refuse offers answer faster than patients who would accept, which leads to a naive prioritization of patients who refuse, letting the organ deteriorate. While TB reports the highest ITE from the benchmarks, its other metrics suggest room for optimization. This is where DynamITE capitalizes on and achieves higher ITEs with lower APTR and CIT.

5.3. Robustness: Patient uncertainty importance.

Experimental setup. One of our key contributions lies in the deliberate incorporation of acceptance and decision timing within DynamITE. To explore the role of acceptance in the DynamITE policy, we examine how varying levels of uncertainty in patient-side decisions impact performance. The acceptance probabilities can be adjusted as follows: $A = \sigma(\frac{\beta(\mathbf{X},\mathbf{O})}{u})$, where $u \in (0, \infty)$ represents the uncertainty parameter. By setting higher values of u, the acceptance probabilities tend to shift closer to 0.5, thereby simulating more uncertain decisions. With the use of u, we evaluate all policies similarly to the patient ranking experiments described in Section 5.2.

Results. Figure 3 shows policy performance in function of uncertainty. Given the low acceptance rate, a higher uncertainty will, on average, increase acceptance rates, while a lower uncertainty will have the opposite effect. For uncertainty values which are not too far from the base value of 1, DynamITE outperforms other policies. However, in further regions, DynamITE begins to lose its edge as its acceptance estimator becomes less accurate.

APTR, CIT and nonuse in function of patient uncertainty. In figure 3 we report performance of the different policies on APTR, CIT and nonuse. For APTR, uncertainty shifts seem to only significantly affect MinTime, as the uncertainty increases MinTime becomes a better policy overall. In terms of both CIT and nonuse, all policies improve significantly with a higher uncertainty.

Given that the average acceptance rate is low (OPTN and SRTR, 2024), increasing uncertainty will increase this acceptance rate but it will also increase decision times. For this reason, it is not evident what to expect from these experiments. However it seems that while the performance of non-ITE-based policies increases with an increase of uncertainty, ITE-based policies tend to perform relatively better when uncertainty levels are low.

Figure 5 in appendix C shows the correlations between metrics across different uncertainty levels for all policies. For both DynamITE and TB, there is a strong negative correlation between ITE and APTR. CIT and nonuse are positively correlated in all policies, especially MaxAcc and MELD, highlighting the importance of minimizing delays. All policies exhibit a negative correlation between APTR and nonuse. DynamITE shows negative correlations between ITE and CIT (-0.57) and between ITE and APTR (-0.81), indicating that its strategy effectively prioritizes patients who both accept quickly and derive significant benefit, reducing CIT and improving outcomes.

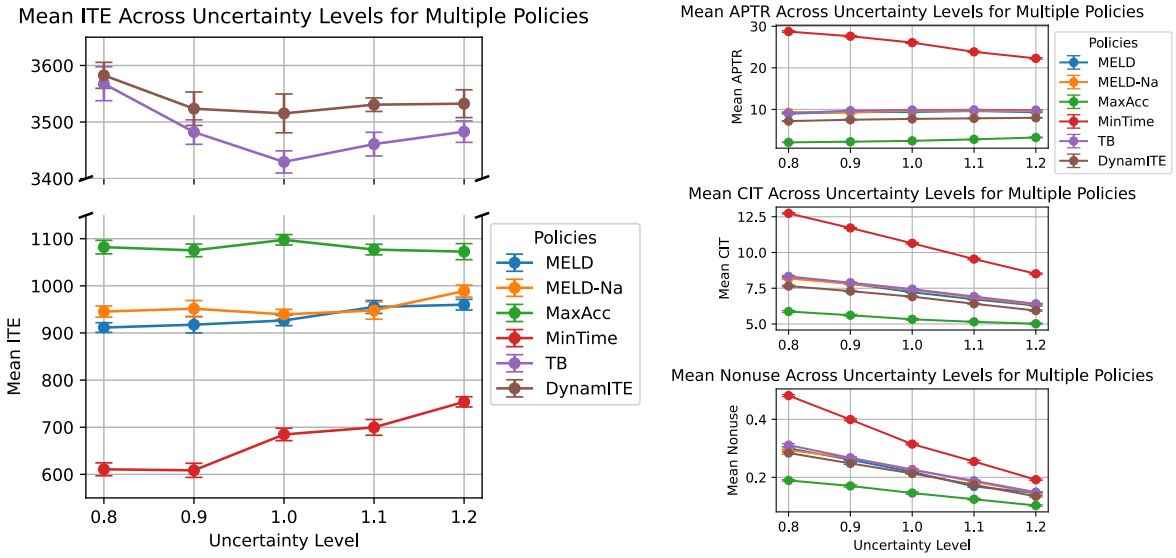

Figure 3: ITE-based performance of policies for different levels of uncertainty, over 10 different runs of each KDE generated scenario (left). Performance of policies across different levels of uncertainty in terms of APTR, CIT and nonuse (right). Error bars are 95% confidence intervals.

6. Discussion

DynamITE's limitations. DynamITE uses estimators to construct an approximated optimization space and objective. Being explicitly defined, DynamITE's objective and constraints can be adjusted for more complex operational settings. The assumption of having access to accurate estimations for potential outcomes might not hold in all cases. These estimators still learn from observational data and rely on causal assumptions, some of which can only be can only be ensured with domain knowledge. Like with all medical devices, both internal and external validation are crucial to ensure that the models do not suffer from any biasses. Furthermore, as distributional shifts might occur over time, a system like DynamITE should be used with active learning mechanisms. Lastly, ethical considerations must be addressed when implementing a policy like DynamITE. While optimizing for overall benefit is desirable, care must be taken to ensure that the algorithm does not inadvertently disadvantage certain patient groups or exacerbate existing disparities in organ allocation. As proposed in other work (Bertsimas et al., 2013, 2020; Papalexopoulos et al., 2022), the desired ethical behavior can be incorporated through the formulation of DynamITE's objective and constraints.

DynamITE through the lens of ML. DynamITE represents a novel approach in organ allocation that incorporates both patient acceptance, decision timing, and dynamic updates to organ quality. In general, moving toward computational models that more closely reflect the complexities of real-world operational and clinical environments represents a significant step forward. Future work could explore strategic decision-making by patients based on historic acceptance data and extend DynamITE to all relevant organ types.

DynamITE through a clinical lens. Late and repeated turndowns of organ offers negatively impact organ quality by increasing cold ischemia time (CIT). DynamITE shows that explicitly modeling offer acceptance and decision time dynamics can increase both the placement efficiency and overall benefit of match-runs. This offers new perspectives for reducing the reliance on out-of-sequence offering, and thereby make allocation more just and transparent. Finally, reducing the average rank of the accepting patient eases the operational burden on the healthcare system by decreasing the number of organ matches that need to be evaluated.

References

Elisa Allen, Rhiannon Taylor, Alexander Gimson, and Douglas Thorburn. Transplant benefit-based offering of deceased donor livers in the United Kingdom. *Journal of Hepatology*, 81(3):471–478, September 2024. ISSN 0168-8278. doi: 10.1016/j.jhep.2024.03.020. URL http://dx.doi.org/10.1016/j.jhep.2024.03.020. Publisher: Elsevier BV.

Barış Ata, Anton Skaro, and Sridhar Tayur. Organjet: Overcoming geographical disparities in access to deceased donor kidneys in the united states. *Management Science*, 63(9):2776–2794, 2017.

Jeroen Berrevoets, James Jordon, Ioana Bica, Mihaela van der Schaar, et al. Organite: Optimal transplant donor organ offering using an individual treatment effect. *Advances in neural information processing systems*, 33:20037–20050, 2020.

Jeroen Berrevoets, Ahmed Alaa, Zhaozhi Qian, James Jordon, Alexander ES Gimson, and Mihaela Van Der Schaar. Learning queueing policies for organ transplantation allocation using interpretable counterfactual survival analysis. In *International Conference on Machine Learning*, pages 792–802. PMLR, 2021.

Dimitris Bertsimas, Vivek F Farias, and Nikolaos Trichakis. Fairness, efficiency, and flexibility in organ allocation for kidney transplantation. *Operations Research*, 61(1):73–87, 2013.

Dimitris Bertsimas, Jerry Kung, Nikolaos Trichakis, David Wojciechowski, and Parsia A Vagefi. Accept or decline? an analytics-based decision tool for kidney offer evaluation. *Transplantation*, 101 (12):2898–2904, 2017.

Dimitris Bertsimas, Theodore Papalexopoulos, Nikolaos Trichakis, Yuchen Wang, Ryutaro Hirose, and Parsia A Vagefi. Balancing efficiency and fairness in liver transplant access: tradeoff curves for the assessment of organ distribution policies. *Transplantation*, 104(5):981–987, 2020.

John M. Cecka. The unos scientific renal transplant registry–2000. *Clinical Transplants*, pages 1–18, 2000.

Agnes Debout, Yohann Foucher, Katy Trébern-Launay, Christophe Legendre, Henri Kreis, Georges Mourad, Valérie Garrigue, Emmanuel Morelon, Fanny Buron, Lionel Rostaing, Nassim Kamar, Michèle Kessler, Marc Ladrière, Alexandra Poignas, Amina Blidi, Jean-Paul Soulillou, Magali Giral, and Etienne Dantan. Each additional hour of cold ischemia time significantly increases the risk of graft failure and mortality following renal transplantation. *Kidney International*, 87(2): 343–349, February 2015. ISSN 0085-2538. doi: 10.1038/ki.2014.304. URL http://dx.doi.org/10.1038/ki.2014.304. Publisher: Elsevier BV.

T.M. Egan, S. Murray, R.T. Bustami, T.H. Shearon, K.P. McCullough, L.B. Edwards, M.A. Coke, E.R. Garrity, S.C. Sweet, D.A. Heiney, and F.L. Grover. Development of the new lung allocation system in the united states. *American Journal of Transplantation*, 6(5):1212–1227, May 2006. ISSN 1600-6135. doi: 10.1111/j.1600-6143.2006.01276.x. URL http://dx.doi.org/10.1111/j.1600-6143.2006.01276.x. Publisher: Elsevier BV.

David S. Goldberg, Benjamin French, James D. Lewis, Frank I. Scott, Ronac Mamtani, Richard Gilroy, Scott D. Halpern, and Peter L. Abt. Liver transplant center variability in accepting organ offers and its impact on patient survival. *Journal of Hepatology*, 64(4):843–851, April 2016. ISSN 0168-8278. doi: 10.1016/j.jhep.2015.11.015. URL http://dx.doi.org/10.1016/j.jhep.2015.11.015.

Juan C David Gomez, Amy L Cochran, and Gabriel Zayas-Caban. Unveiling bias in sequential decision making: A causal inference approach for stochastic service systems. *arXiv preprint arXiv:2307.07879*, 2023.

Meredith Hackmann, Rebecca A. English, and Kenneth W. Kizer. Improving Procurement, Acceptance, and Use of Deceased Donor Organs. In *Realizing the Promise of Equity in the Organ Transplantation System*. National Academies Press (US), February 2022. URL https://www.ncbi.nlm.nih.gov/books/NBK580022/.

HRSA. Organ Donation Statistics. Technical report, HRSA (Health Resources and Services Administration), 2023. URL https://www.organdonor.gov/learn/organ-donation-statistics.

S. Ali Husain, Joel T. Adler, and Sumit Mohan. Radical transparency to improve equity in the kidney al-

location system. *Kidney360*, 5(1):121–123, November 2023. ISSN 2641-7650. doi: 10.34067/kid.0000000000000327. URL http://dx.doi.org/10.34067/KID.0000000000000327. Publisher: Ovid Technologies (Wolters Kluwer Health).

Ajay K. Israni, David A. Zaun, Katrina Gauntt, Cory R. Schaffhausen, Cinthia Lozano, Warren T. McKinney, Jonathan M. Miller, and Jon J. Snyder. OPTN/SRTR 2022 annual data report: Deceased organ donation. *American Journal of Transplantation*, 24(2):S457–S488, February 2024. ISSN 1600-6135. doi: 10.1016/j.ajt.2024.01.018. URL http://dx.doi.org/10.1016/j.ajt.2024.01.018. Publisher: Elsevier BV.

Sang-Phil Kim, Diwakar Gupta, Ajay K Israni, and Bertram L Kasiske. Accept/decline decision module for the liver simulated allocation model. *Health care management science*, 18:35–57, 2015.

W Ray Kim, Scott W Biggins, Walter K Kremers, Russell H Wiesner, Patrick S Kamath, Joanne T Benson, Erick Edwards, and Terry M Therneau. Hyponatremia and mortality among patients on the liver-transplant waiting list. *New England Journal of Medicine*, 359(10):1018–1026, 2008.

Kristen L. King, Sulemon G. Chaudhry, Lloyd E. Ratner, David J. Cohen, S. Ali Husain, and Sumit Mohan. Declined offers for deceased donor kidneys are not an independent reflection of organ quality. *Kidney360*, 2(11):1807–1818, November 2021. ISSN 2641-7650. doi: 10.34067/kid.0004052021. URL http://dx.doi.org/10.34067/KID.0004052021. Publisher: Ovid Technologies (Wolters Kluwer Health).

Kristen L. King, S. Ali Husain, Adler Perotte, Joel T. Adler, Jesse D. Schold, and Sumit Mohan. Deceased donor kidneys allocated out of sequence by organ procurement organizations. *American Journal of Transplantation*, 22(5):1372–1381, May 2022. ISSN 1600-6135. doi: 10.1111/ajt.16951. URL http://dx.doi.org/10.1111/ajt.16951. Publisher: Elsevier BV.

Xun Luo, Joseph Leanza, Allan B Massie, Jacqueline M Garonzik-Wang, Christine E Haugen, Sommer E Gentry, Shane E Ottmann, and Dorry L Segev. Meld as a metric for survival benefit of liver transplantation. *American Journal of Transplantation*, 18(5):1231–1237, 2018.

Michael Malinchoc, Patrick S Kamath, Fredric D Gordon, Craig J Peine, Jeffrey Rank, and Pieter CJ Ter Borg. A model to predict poor survival in patients undergoing transjugular intrahepatic portosystemic shunts. *Hepatology*, 31(4):864–871, 2000.

Sumit Mohan, Mariana C. Chiles, Rachel E. Patzer, Stephen O. Pastan, S. Ali Husain, Dustin J. Carpenter, Geoffrey K. Dube, R. John Crew, Lloyd E. Ratner, and David J. Cohen. Factors leading to the discard of deceased donor kidneys in the United States. *Kidney International*, 94(1):187–198, July 2018. ISSN 0085-2538. doi: 10.1016/j.kint.2018.02.016. URL http://dx.doi.org/10.1016/j.kint.2018.02.016. Publisher: Elsevier BV.

Michael S. Mulvihill, Hui J. Lee, Jeremy Weber, Ashley Y. Choi, Morgan L. Cox, Babatunde A. Yerokun, Muath A. Bishawi, Jacob Klapper, Maragatha Kuchibhatla, and Matthew G. Hartwig. Variability in donor organ offer acceptance and lung transplantation survival. *The Journal of Heart and Lung Transplantation*, 39(4):353–362, April 2020. ISSN 1053-2498. doi: 10.1016/j.healun.2019.12.010. URL http://dx.doi.org/10.1016/j.healun.2019.12.010. Publisher: Elsevier BV.

James Neuberger, Alex Gimson, Mervyn Davies, Murat Akyol, John O'Grady, Andrew Burroughs, Mark Hudson, UK Blood, et al. Selection of patients for liver transplantation and allocation of donated livers in the uk. *Gut*, 57(2):252–257, 2008.

OPTN. OPTN policies. https://optn.transplant.hrsa.gov/media/eavh5bf3/optn_policies.pdf, 2021. Accessed: 24-08-31.

OPTN and SRTR. Optn/srtr 2022 annual data report. Technical report, U.S. Department of Health and Human Services, Health Resources and Services Administration, 2024. URL http://srtr.transplant.hrsa.gov/annual_reports/Default.aspx. Accessed: 2024-08-22.

Theodore P Papalexopoulos, Dimitris Bertsimas, I Glenn Cohen, Rebecca R Goff, Darren E Stewart, and Nikolaos Trichakis. Ethics-by-design: efficient, fair and inclusive resource allocation using machine learning. *Journal of Law and the Biosciences*, 9(1):lsac012, 2022.

Roger Ratcliff and Jeffrey N Rouder. Modeling response times for two-choice decisions. *Psychological science*, 9(5):347–356, 1998.

Burhaneddin Sandikci, Sait Tunc, and Bekir Tanriover. A new simulation model for kidney transplantation in the united states. In *2019 Winter Simulation Conference (WSC)*. IEEE, December 2019. doi: 10.1109/wsc40007.2019.9004914. URL http://dx.doi.org/10.1109/WSC40007.2019.9004914.

SRTR. *KPSAM 2015 User Guide*, 2015a. URL https://www.srtr.org/media/1295/kpsam-2015-user-guide.pdf. Accessed: 2024-08-31.

SRTR. *TSAM 2015 User Guide*, 2015b. URL https://www.srtr.org/media/1294/tsam-2015-user-guide.pdf. Accessed: 2024-08-31.

SRTR. *LSAM 2019 User Guide*, 2019. URL https://www.srtr.org/media/1361/LSAM-2019-User-Guide.pdf. Accessed: 2024-08-31.

Darren E. Stewart, Victoria C. Garcia, John D. Rosendale, David K. Klassen, and Bob J. Carrico. Diagnosing the decades-long rise in the deceased donor kidney discard rate in the united states. *Transplantation*, 101(3):575–587, March 2017. ISSN 0041-1337. doi: 10.1097/tp.0000000000001539. URL http://dx.doi.org/10.1097/TP.0000000000001539. Publisher: Ovid Technologies (Wolters Kluwer Health).

Maurits T. Vinkers, Jacqueline M. Smits, Ineke C. Tieken, Jan de Boer, Dirk Ysebaert, and Axel O. Rahmel. Kidney donation and transplantation in eurotransplant 2006–2007: Minimizing discard rates by using a rescue allocation policy. *Progress in Transplantation*, 19(4):365–370, December 2009. ISSN 2164-6708. doi: 10.1177/152692480901900414. URL http://dx.doi.org/10.1177/152692480901900414.

Andrew Wey, Nicholas Salkowski, Bertram L. Kasiske, Ajay K. Israni, and Jon J. Snyder. Influence of kidney offer acceptance behavior on metrics of allocation efficiency. *Clinical Transplantation*, 31(9), August 2017. ISSN 1399-0012. doi: 10.1111/ctr.13057. URL http://dx.doi.org/10.1111/ctr.13057. Publisher: Wiley.

Alan D. White, Heather Roberts, Clare Ecuyer, Kathryn Brady, Samir Pathak, Brendan Clark, Lutz H. Hostert, Magdy S. Attia, Matthew Wellberry-Smith, Alex Hudson, and Niaz Ahmad. Impact of the new fast track kidney allocation scheme for declined kidneys in the United Kingdom. *Clinical Transplantation*, 29(10):872–881, September 2015. ISSN 1399-0012. doi: 10.1111/ctr.12576. URL http://dx.doi.org/10.1111/ctr.12576. Publisher: Wiley.

Russell Wiesner, Erick Edwards, Richard Freeman, Ann Harper, Ray Kim, Patrick Kamath, Walter Kremers, John Lake, Todd Howard, Robert M. Merion, Robert A. Wolfe, and Ruud Krom. Model for end-stage liver disease (MELD) and allocation of donor livers. *Gastroenterology*, 124(1):91–96, January 2003. ISSN 0016-5085. doi: 10.1053/gast.2003.50016. URL http://dx.doi.org/10.1053/gast.2003.50016. Publisher: Elsevier BV.

Nicholas L. Wood, Douglas B. Mogul, Emily R. Perito, Douglas VanDerwerken, George V. Mazariegos, Evelyn K. Hsu, Dorry L. Segev, and Sommer E. Gentry. Liver simulated allocation model does not effectively predict organ offer decisions for pediatric liver transplant candidates. *American Journal of Transplantation: Official Journal of the American Society of Transplantation and the American Society of Transplant Surgeons*, 21(9):3157–3162, September 2021. ISSN 1600-6143. doi: 10.1111/ajt.16621.

Jinsung Yoon, Ahmed M Alaa, Martin Cadeiras, and Mihaela Van Der Schaar. Personalized donor-recipient matching for organ transplantation. In *Thirty-First AAAI Conference on Artificial Intelligence*, 2017.

Yunwei Zhang, Anne Hu, Yingxin Lin, Yue Cao, Samuel Muller, Germaine Wong, and Jean Yee Hwa Yang. simkap: simulation framework for the kidney allocation process with decision making model. *Scientific Reports*, 13(1):16367, 2023.

Appendix A. Additional experiments

A.1. Search algorithm importance.

Experimental setup. DynamITE uses a search to optimize 12. In our experiments, we investigated how different configurations of the local search algorithm affect the performance of DynamITE. Specifically, we tested various combinations of the parameters `iterations`, `top_k`, and `accuracy` on 100 different KDE generated scenarios. The parameter `iterations` controls how many times DynamITE iterates over the ranking to perform adjacent swaps. The `top_k` parameter determines the number of top-ranked patients considered for optimization, and `accuracy` defines the fraction of the ranking used to approximate the objective function $\kappa(\mathbf{R}, \mathbf{O}_1)$. A more detailed description of these search parameters can be found in appendix B. The local search is run on an Intel Core i7-1265U processor.

Results. Table 3 summarizes the results of these experiments, with the configuration parameters presented as individual columns. We report the average run time, the average estimated κ (days gained) as calculated by DynamITE using its internal estimations, and the average true κ (days gained) computed using the synthetic functions. The configuration with `iterations = 0` corresponds to no search (i.e., the initial ranking without any local search optimization).

The results demonstrate that more extensive search configurations generally lead to improved true ITE gains. For instance, increasing the number of iterations and the `top_k` value tends to result in higher ITE, albeit at the cost of increased computational time. Notably, the configuration with `iterations = 3`, `top_k = 15`, and `accuracy = 0.40` achieves the highest average true ITE of 2930.50 days but also requires the longest average run time of approximately 22.69 seconds.

These findings indicate that while a more exhaustive search can enhance the performance of DynamITE by finding better patient rankings, there is a trade-off between computational efficiency and the quality of the solution. In practice, the choice of search parameters can be tailored based on the available computational resources and the acceptable time constraints for the allocation process.

A.2. Positivity check.

Experimental setup. Consider $\hat{s}_{\mathbf{O}\neq\emptyset}$ and $\hat{s}_{\mathbf{O}=\emptyset}$ as the estimated probability that a patient does and does not receive a transplant respectively. We test whether a relaxed version of the positivity assumption 1 holds by plotting a histogram of the highest estimated propensity score $\hat{s}_{max} = \max\{\hat{s}_{\mathbf{O}\neq\emptyset}, \hat{s}_{\mathbf{O}=\emptyset}\}$ for each observed patient.

Results. Figure 4 shows the histograms for both the real and simulated data, in both cases, positivity is violated as there are many instances with an $\hat{s}_{max}$ close to 1.

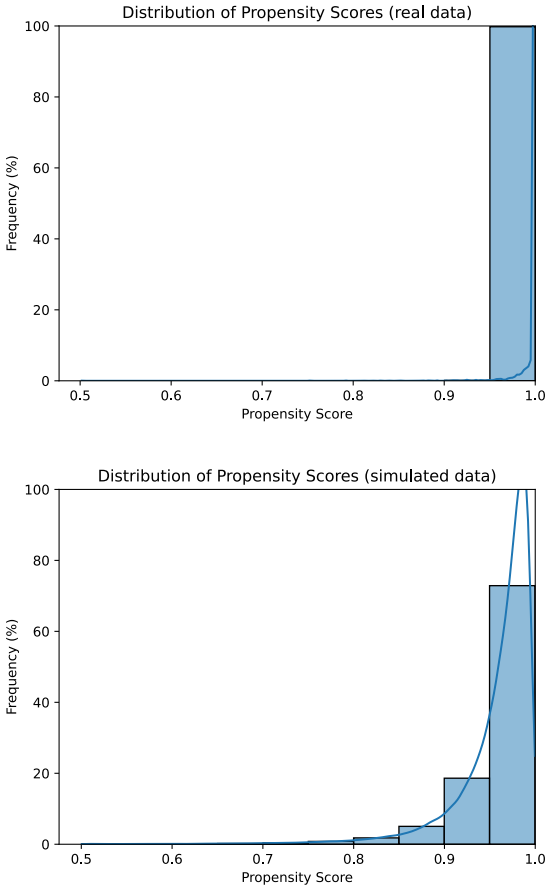

Figure 4: Histograms for frequencies of propensity scores for receiving an organ given the patient features in both real (upper) data and data from simulated matches (lower). Propensity scores are estimated using a linear regression model. The blue curves are KDE approximations of the frequencies.

Table 3: Performance of DynamITE with different local search configurations over 100 KDE generated scenarios. The first row (`iterations = 0`) represents the baseline without search. For each tested configuration tuple (`iterations`, `top_k`, `accuracy`) the run time, estimated κ, and true κ are shown.

Iterations	Top_k	Accuracy	Run Time (s)	Estimated κ (days)	True κ (days)
0	0	.00	0.55	n.a.	2853.58
1	5	.30	**3.34**	2695.41	2902.07
1	15	.30	8.52	2701.25	2902.48
1	5	.40	3.66	2710.54	2902.77
1	15	.40	9.33	2724.00	2902.99
2	5	.30	6.71	2709.73	2919.14
2	5	.40	6.85	2724.89	2919.48
2	15	.30	18.48	2721.57	2922.43
2	15	.40	18.87	2745.26	2922.48
3	5	.30	7.30	2714.44	2924.45
3	5	.40	7.35	2729.60	2924.79
3	15	.30	22.22	2729.68	2930.04
3	15	.40	22.69	**2753.28**	**2930.50**

Appendix B. Supplemental content for experiments

B.1. Acceptance and decision time estimation.

Synthetic acceptance function. In section 5.1 we define how we use the function $\beta(\mathbf{X}, \mathbf{O})$ to model acceptance probabilities. Specifically, we define function $\beta(\mathbf{X}, \mathbf{O})$ as follows:

$$\begin{aligned}\beta(\mathbf{X}, \mathbf{O}) := h_1 \text{MELD}(\mathbf{X}) - h_2 \mathbf{O}[\text{CIT}] \\ - h_3 \mathbb{I}[|\mathbf{X}[\text{AGE}] - \mathbf{O}[\text{AGE}]| \leq 30] \\ - h_4 \mathbb{I}[|\mathbf{X}[\text{BMI}] - \mathbf{O}[\text{BMI}]| \leq 5] \\ + U_A \end{aligned} \tag{20}$$

Here, MELD($\mathbf{X}$) returns the MELD score of patient $\mathbf{X}$, capped between 0 and 40, and U_A is a uniform distribution between $[-0.5; 0.5]$. We took into consideration conditions based on the age and BMI differences between donor organ and patient. Hyperparameters h_1, h_2, h_3, h_4 have been tuned manually together with hyperparameters from the decision time function such that observed acceptance rates and cold ischemic times would coincide with the actual statistics. We find the following hyperparameters to model acceptance appropriately and resulting in the statistics: $h_1 = 0.01, h_2 = 0.15, h_3 = 0.22, h_4 = 0$. So we find it is best to leave BMI compatibility out of the acceptance function.

In our acceptance function, we take the MELD score as an urgency metric (Luo et al., 2018), we model the impact of CIT on acceptance and take some organ-patient compatibility (AGE and BMI) factors into account.

Synthetic decision time function. In section 5.1 we introduce a synthetic decision time function. This function has been constructed based on the experiments of Ratcliff and Rouder (1998). The interval of the uniform distribution U_T has been tuned and set to $[0, 0.4]$. U_T is always positive as it involves operational overhead time of sending and receiving the organ offer notification and corresponding answer. Currently, the maximum amount of time to respond is 2 hours (OPTN, 2021), this is used as constraint to find λ, which eventually is set to -8. During simulated runs, for both the estimations and the simulations, if T is above 2 hours, then it gets capped at 2 hours and the corresponding answer will be a refusal.

PatientNet hyperparameters. We tuned the models in table 1 and trained our PatientNet model with the hyperparameters listed in table 4.

B.2. Patient ranking policies.

Generated scenarios. For the results in table 2 we generate 1000 initial organs using KDEs and setting $\mathbf{O}[\text{CIT}] := 0$. Next for each of these organs we generate a waitlist $\mathcal{X}_Q$ of size 50 containing KDE gen-

Table 4: PatientNet Hyperparameters

Component	Hyperparameters
Shared Representation $\Phi_{\theta_\Phi}(\mathbf{X}, \mathbf{O})$	Dense(64, L2), LeakyReLU Dense(32, L2), LeakyReLU
Acceptance Head $A_{\theta_A}(\phi)$	Dense(1), Sigmoid Activation
Decision Time Head $T_{\theta_T}(\phi)$	Dense(1), ReLU Activation
Task Loss Weight γ	1
Training Parameters	Maximum Epochs: 1000 Patience: 50

erated patients. Each organ-waitlist pair $(\mathbf{O}_1, \mathcal{X}_Q)$ represents a generated scenario. We let each policy handle each scenario for 10 different runs.

Organ nonuse. In our experiments, a nonused organ is an organ that is refused by the last patient of the ranking. In the case of nonuse, the organ will not result in an ITE.

Dyna scores. In expression 4.3 we introduced the dyna scores. Intuitively, the Dyna score incorporates the accept-to-decision-time ratio and the benefit (ITE) of the patients to rank them. If the score would only take into account the benefit of the patients, then it would simplify to the TB policy. By taking the ratio into consideration the policy promotes patients who are likely to accept quickly and demotes patients who are likely to refuse slowly. As such, the Dyna scores balance allocating the organ quickly (reducing CIT) and allocating the organ to the patient who would benefit the most conditional upon acceptance. We manually tuned hyperparameters $\alpha_A, \alpha_T, \alpha_\tau$ on a different set of generated organ-waitlist pairs. For experiments, we used $\alpha_A = 0.6, \alpha_T = 1, \alpha_\tau = 0.7$.

DynamITE. Results for DynamITE in table 2 are shown with and without the search algorithm. For the search algorithm we use a local search based on local swaps. This local search must constantly approximate κ as it is optimizing it as objective. However, approximating $\kappa(\mathbf{R}, \mathbf{O}_1)$ is very computationally demanding as it requires 3 estimations ($\hat{A}_k$, $\hat{\tau}_k$ and $\hat{\mathbf{O}}_{k+1}$) for each patient in $\mathcal{X}_Q$. Moreover, these estimations are interdependent as the estimations for the patient at rank k can only be done once we already have the estimations for the patient at rank $k-1$, inhibiting approaches that would exploit parallelism.

For this reason, we relax the search by adding tunable search parameters:

- `iterations`: how many times DynamITE goes over the ranking in ascending order and tries to perform adjacent swaps. In experiment 5.2, this value is set to 1.
- `top_k`: determines over how many patients DynamITE should optimize. These will be the patients with ranks 1 up to *top_k*. We consider patients starting from the top as a change at the top in the ranking is expected to have a bigger impact than a change further down the ranking. This is because a swap between two patients at ranks k and $k+1$ will change acceptance probabilities, decision times and ITE of all patients at ranks larger than $k+1$, while leaving patients with ranks smaller than k completely unaffected. In experiment 5.2, this value is set to 5.
- `accuracy`: up to which patient $\kappa(\mathbf{R}, \mathbf{O}_1)$ is computed. In expression 11, K will be set to the closest integer to $accuracy * K$ resulting in an incomplete estimation of $\kappa(\mathbf{R}, \mathbf{O}_1)$. In experiment 5.2 we set this value to 0.4, resulting in $\kappa(\mathbf{R}, \mathbf{O}_1)$ being estimated for only the first 40% of patients.

These parameters have been set low for computational reasons. Nonetheless, this simple search significantly improves DynamITE's performance as shown in table 2, resulting in a 67 days average improvement in ITE for each allocated organ.

Appendix C. Additional figures and tables

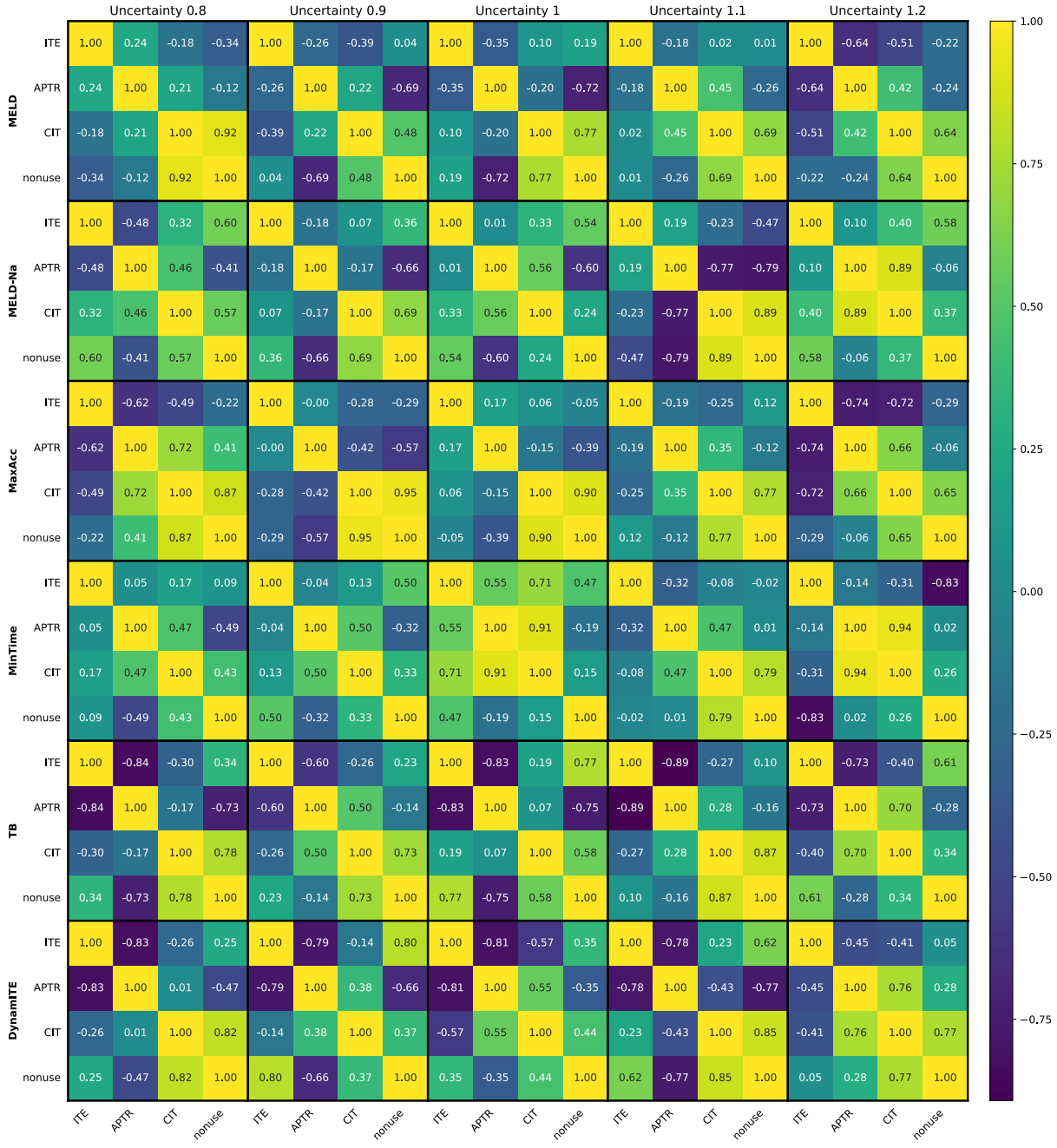

Figure 5: Correlations between ITE, APTR, CIT and Nonuse across different uncertainty levels for all policies

Patient Features	
GENDER	recipient gender
DAYSWAIT_CHRON	days on liver waiting list
ETHCAT	recipient ethnicity category
INIT_AGE	age in years at time of listing
INIT_ALBUMIN	initial waiting list albumin
INIT_ASCITES	initial waiting list ascites
INIT_BMI_CALC	calculated candidate bmi at listing
INIT_BILIRUBIN	initial waiting list bilirubin
INIT_INR	initial waiting list inr
INIT_SERUM_CREAT	initial waiting list serum creatinine
INIT_SERUM_SODIUM	initial waiting list serum sodium
HGT_CM_CALC	calculated recipient height (cm)
WGT_KG_CALC	calculated recipient weight (kg)
DIAG	recipient primary diagnosis
Organ Features	
AGE_DON	donor age (yrs)
ALCOHOL_HEAVY_DON	ddr heavy alcohol use (heavy= 2+ drinks/day) (y/n/u)
BMI_DON_CALC	donor bmi - pre/at donation calculated
COD_CAD_DON	deceased donor-cause of death
COLD_ISCH	total cold ischemic time (hours)
ETHCAT_DON	donor ethnicity category
HGT_CM_DON_CALC	calculated donor height (cm)
HIST_CANCER_DON	deceased donor-history of cancer (y/n)
HIST_CIG_DON	deceased donor-history of cigarettes in past (more than 20 pack yrs)
GENDER_DON	donor gender
NON_HRT_DON	deceased donor-non-heart beating donor

Table 5: Considered features from the UNOS dataset (Cecka, 2000) to represent patients and organs.

Table 6: Summary of notations used in section 3

Symbol	Definition	Description
$\mathcal{X}$	Patient space	Set of all possible patients, $\mathcal{X} \subset \mathbb{R}^d$
$\mathcal{O}$	Organ space	Set of all possible organs, $\mathcal{O} \subset \mathbb{R}^e$
$\mathbf{X}$	Patient vector	A patient, $\mathbf{X} \in \mathcal{X}$
$\mathbf{O}$	Organ vector	An organ, $\mathbf{O} \in \mathcal{O} \cup \{\emptyset\}$; $\emptyset$ represents no organ
A	Offer response	Patient's response to an organ offer, $A \in \{0, 1\}$; $A = 1$ if accepted, $A = 0$ if refused
T	Decision time	Time between offer and acceptance, $T \in \mathbb{R}_+$
$\mathcal{P}(\mathcal{X})$	Powerset of $\mathcal{X}$	Set of all subsets of $\mathcal{X}$
$\mathcal{X}_Q$	Waiting list	A set of patients on the waitlist, $\mathcal{X}_Q \subset \mathcal{P}(\mathcal{X})$
K	Waitlist size	Number of patients on the waitlist, $K = \lvert\mathcal{X}_Q\rvert$
$\mathrm{Sym}(\mathcal{X}_Q)$	Symmetric group	Set of all permutations (rankings) of $\mathcal{X}_Q$
$\mathbf{R}$	Patient ranking	A ranking of waitlisted patients, $\mathbf{R} \in \mathrm{Sym}(\mathcal{X}_Q)$
k	Sequence number	Position in the ranking, $k \in \mathbb{Z}^+$, $1 \leq k \leq K$
$\mathbf{X}_k$	Patient at rank k	The k-th patient in the ranking, $\mathbf{X}_k \in \mathcal{X}_Q$
$\mathbf{O}_k$	Organ at step k	Organ offered to $\mathbf{X}_k$
A_k	Response at rank k	Acceptance ($A_k = 1$) or refusal ($A_k = 0$) by $\mathbf{X}_k$
T_k	Decision time at rank k	Time taken by $\mathbf{X}_k$ to respond
P	Acceptance rank	Rank at which the organ is accepted, $A_P = 1$
$\mathbf{X}_P$	Accepting patient	Patient who accepts the organ offer
$Y^{\mathbf{o}}$	Potential outcome	Life expectancy for $\mathbf{X}$ when receiving organ $\mathbf{o}$
Y	Observed outcome	Actual life expectancy, $Y = Y^{\mathbf{O}}$
$\tau(\mathbf{X}, \mathbf{O})$	ITE	Expected benefit of $\mathbf{X}$ receiving $\mathbf{O}$, $\tau(\mathbf{X}, \mathbf{O}) = \mathbb{E}[Y^{\mathbf{O}} - Y^{\emptyset} \mid \mathbf{X}]$
τ_k	ITE at rank k	ITE for patient $\mathbf{X}_k$, $\tau_k = \tau(\mathbf{X}_k, \mathbf{O}_k)$
$\tau(\mathbf{R}, \mathbf{O}_1)$	Ranking benefit	Actual benefit of ranking $\mathbf{R}$, $\tau(\mathbf{R}, \mathbf{O}_1) = \sum_{k=1}^{K} \tau_k \mathbb{I}[A_k = 1]$
$\kappa(\mathbf{R}, \mathbf{O}_1)$	Expected benefit	Expected benefit from ranking $\mathbf{R}$ and initial organ $\mathbf{O}_1$, $\kappa(\mathbf{R}, \mathbf{O}_1) = \mathbb{E}[\tau(\mathbf{R}, \mathbf{O}_1)]$
$\mathcal{D}$	Dataset	Set of historical offers and responses, $\mathcal{D} = \{((\mathbf{x}_k, \mathbf{o}_k, a_k, t_k) : k = 1, \ldots, P_i) : i = 1, \ldots, N\}$
N	Number of offers	Total number of initial organ offers
$p(\mathbf{X})$	Patient distribution	Probability distribution over patient attributes
$p(\mathbf{O}_1)$	Initial organ distribution	Probability distribution over initial organ attributes
π	Policy	A function defining the patient ranking
π_{obs}	Observed policy	Policy used to generate the dataset $\mathcal{D}$
$\hat{\pi}$	Estimated policy	The policy to be identified, $\hat{\pi} : \mathcal{X}_Q \times \mathcal{O} \to \mathrm{Sym}(\mathcal{X}_Q)$
$\mathbb{E}[\kappa]$	Expected benefit	Expected value of κ, averaged over $p(\mathbf{X})$ and $p(\mathbf{O})$
$\mathbb{I}[\cdot]$	Indicator function	Equals 1 if the condition is true, 0 otherwise